

Fig. 2. Digitally-assisted analog mitigation of frequency-modulated interference [5] applied to recover GNSS signals-of-interest.

II. NARROWBAND INTERFERENCE MITIGATION

The interference mitigation method used and analyzed herein has previously been published in [5]. In essence, the method is based on using an auxiliary transmit chain, similarly to some of the proposed FD radio architectures [10], to suppress the interference in the received signal before quantization as illustrated in Fig. 2. The implementation requires estimating the instantaneous frequency of the narrowband interference signal $x(n)$ and constructing a digital representation $\hat{x}(n)$ of the interference such that it exactly follows the estimated frequencies. Of course, it is only possible to precisely estimate the instantaneous frequency of the interference as long as the interference is sufficiently more powerful than the signal-of-interest. However, this is exactly the situation this work focuses on with powerful co-located interference. Also, when considering GNSS as signals-of-interest, estimation of the interference's instantaneous frequency is aided by the spread spectrum nature of the GNSS signals.

In order to obtain an interference-free version of the signal-of-interest $s(n)$, the input signal $s(n) + x(n)$ is employed as the reference signal for the adaptive filter. The estimated jamming signal $\hat{x}(n)$, which is strongly correlated to the actual jamming signal $x(n)$, is employed as the input for the adaptive filter. The adaptive mechanism adjusts the filter coefficients of $W(z)$ in such a manner that the filter output $y(n)$ approximates the jamming signal, thus forcing the error signal $e(n)$ to resemble the signal-of-interest $s(n)$.

The use of adaptive filtering for analog interference mitigation is complicated by the fact that the summation of signals represents radio-frequency (RF) superposition and it is necessary to compensate for the secondary-path transfer function $S(z)$, which includes a digital-to-analog converter (DAC), a power amplifier (PA), a power combiner, a low-noise amplifier (LNA), and an analog-to-digital converter (ADC). Thus, the adaptive filter needs to imitate the secondary-path transfer function $S(z)$ with a transfer function $\hat{S}(z)$ applied to the input [11]. Fortunately, offline modeling can be used to estimate $S(z)$ during an initial training stage as the signal path from the auxiliary transmitter TX_{AUX} to the primary receiver RX can be considered static. Still, due to the computational delays involved in estimating the instantaneous frequency, filtering etc., the system's response is non-causal and the system is capable of effectively canceling only narrowband pseudorandom or periodic interference [11].

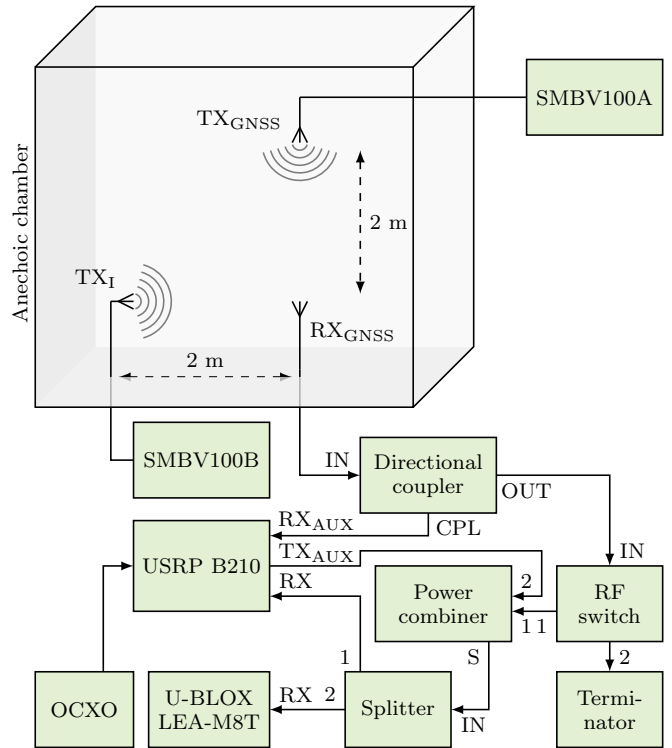


Fig. 3. The setup for measuring the over-the-air performance of the interference mitigation platform using GPS L1 and Galileo E1 as signals-of-interest.

III. EXPERIMENTAL SETUP

The measurement setup is outlined in Fig. 3. The interference mitigation prototype is built using an USRP B210 software-defined radio (SDR) and the prototype's performance is analyzed by using simultaneously a commercial GNSS receiver U-Blox LEA-M8T and an open-source GNSS software-defined receiver (GNSS-SDR) [12] that processes IQ samples from the SDR. The measurements are carried out in an anechoic chamber to avoid interfering with GNSS receivers in the vicinity and to be able to use a controlled GNSS source. A signal generator SMBV100A is used for transmitting GPS L1 C/A and Galileo E1 signals that simulate six satellites with predefined location, time, and power. A separate signal generator SMBV100B is used for transmitting a sinusoidally FM interference with deviation of 125 kHz, modulation rate of 1 kHz, and center frequency of 1575.42 MHz.

An active GPS antenna with 27 dBi gain and 1.5 dB noise figure (Trimble 39265-50) is used to receive the GNSS and interference signals, whereas directional log-periodic antennas are used for transmitting the signals. The signal after interference mitigation is split between the U-Blox receiver and the receiver for GNSS-SDR. The U-Blox receiver logs National Marine Electronics Association (NMEA) and U-Blox proprietary messages. The SDR is used for the interference mitigation but also for recording IQ samples with sampling rate of 4.096 MHz. The sampling rate is chosen to be slightly above an integer multiple of the chipping rate as using a multiple of the chipping rate leads to poor accuracy in the estimation of pseudoranges [13].

For each measurement, 4 min of U-Blox logs and IQ samples are recorded so that both the U-Blox receiver and GNSS-SDR could acquire the position from a cold-start situation. In order to have a fair comparison between the U-Blox receiver and the GNSS-SDR toolbox, the U-Blox receiver is restarted before each measurement. In that way, every U-Blox recording and IQ recording represents a standalone unit for analysis without *a priori* information on satellites' pseudoranges, etc.

IV. EXPERIMENTAL RESULTS

When receiving the combination of a GNSS signal and FM interference, the platform provides about 35 dB of interference suppression as illustrated in Fig. 4 (where GPS cases are omitted as they are very similar to the Galileo ones). Those results closely resemble the previous findings achieved without any signals-of-interest [5]. But does this lead to improvements in GNSS reception? In the following subsections, we provide in-depth analysis into how the interference mitigation affects actual GPS L1 and Galileo E1 reception in the RF front-end, acquisition, tracking, and positioning stages.

A. RF Front-End

The first stage of a GNSS receiver is the RF front-end, which is typically used to filter the input signal down to the bandwidth of interest, downconvert, amplify using automatic gain control (AGC), and finally quantize using an ADC. In-band interference, however, by-passes such filtering and affects the AGC, consequently determining how well the AGC is capable of minimizing quantization errors of the GNSS signals in the ADC. The gain level set by the AGC in the U-Blox receiver with respect to the jammer-to-signal ratio (JSR) is plotted in Fig. 5. It is evident that as the power of the interference increases, the AGC decreases the gain level to prevent from overflowing the ADC, which is exactly the purpose of the AGC. Because AGC is typically the first in line to be affected by adversarial interference, AGC is potentially well suited for interference detection [14].

The U-Blox receiver also features an internal interference detector that provides an interference detection confidence level, although it is unclear, whether the interference indicator takes the AGC information into account in this case. The interference confidence level is plotted alongside the AGC data

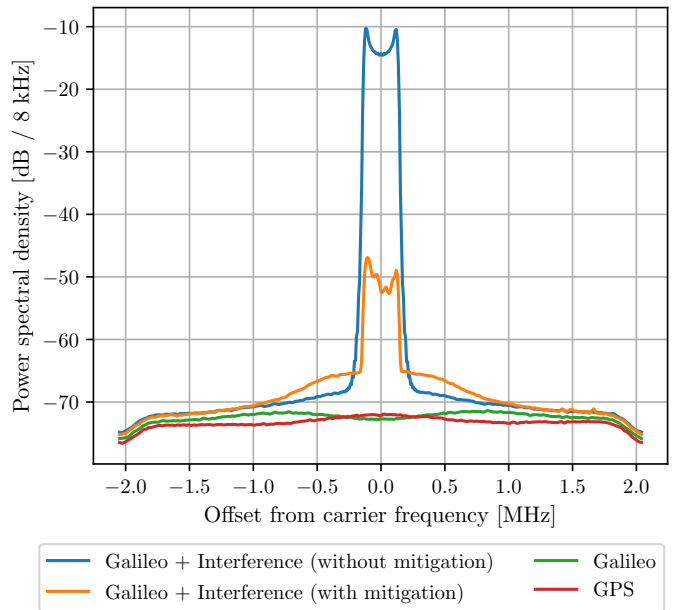


Fig. 4. Power spectral density of the received GNSS and interference signals.

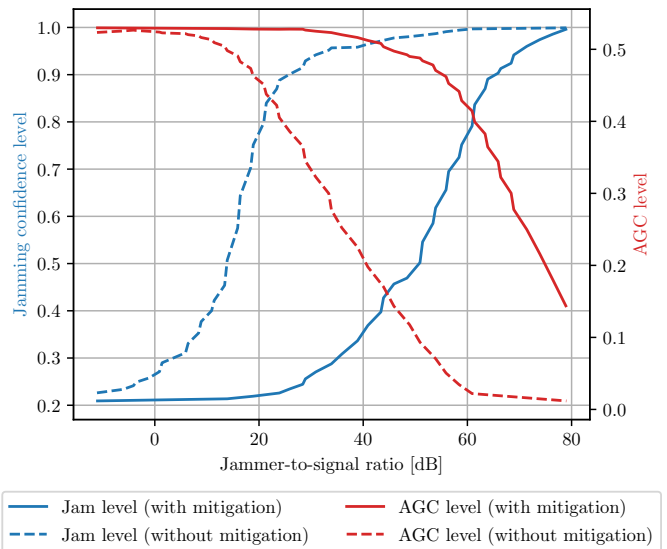


Fig. 5. U-Blox LEA-M8T hardware monitoring results.

in Fig. 5. As the interference power increases so does the interference detection confidence level. The reported AGC level and interference confidence level are not exactly reciprocal, yet both of these metrics seems to be similarly affected by the interference mitigation. Comparing the AGC and interference confidence levels with and without interference mitigation indicates that interference mitigation extends the normal working range of the U-Blox receiver RF front-end by 30 dB to 40 dB. As such, analog interference mitigation might also turn useful for improving the reception quality of systems, for which baseband digital signal processing is not accessible.

B. Acquisition

Acquisition stage is the first digital stage in GNSS reception and it is tasked with detecting the presence of GNSS signals and providing coarse estimates of the signals' code phase and Doppler frequency for the tracking stage [15]. Acquisition is essentially achieved by correlating the received signal with locally generated replicas, which are characterized by specific code delays and Doppler frequencies.

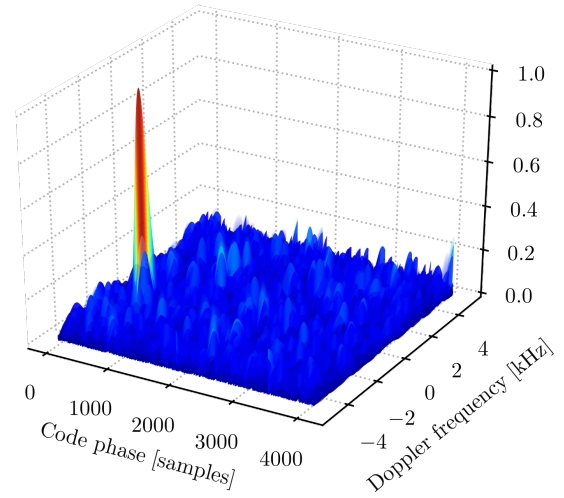
Figure 6 illustrates how the acquisition search space for GPS L1 is affected by interference at JSR of 50 dB with and without interference mitigation. The acquisition search space is calculated using 1 ms of integration time and 2 Hz Doppler frequency step in the GNSS-SDR toolbox. Galileo E1 acquisition search space exhibits similar behaviour and has not been included for brevity.

Without interference (cf. Fig. 6a), a single predominant peak appears in the cross-ambiguity function (CAF) that indicates the presence of the signal and its code delay and Doppler shift. With interference, the separation between the cross-correlation peak and the noise floor decreases drastically (cf. Fig. 6b), leading to increased probability of false alarms or even providing inaccurate code phase and Doppler frequency estimates [16]. Interference mitigation improves the CAF significantly (cf. Fig. 6c) and a single dominant peak is distinguishable from the noise floor again.

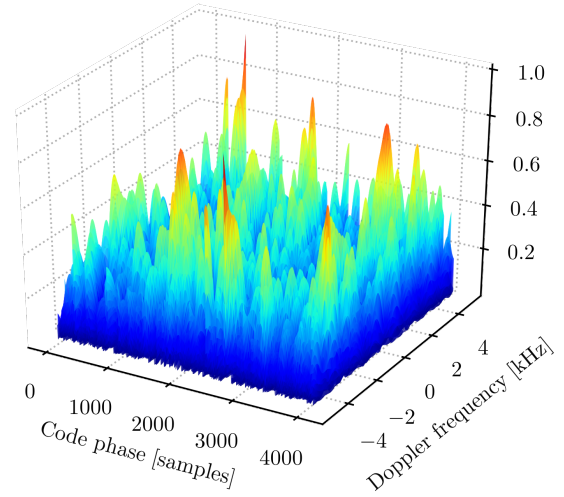
C. Tracking

Tracking stage uses the coarse estimates from the acquisition stage to provide fine estimates of the GNSS signal parameters, which in turn are used for generating pseudoranges [16]. The tracking stage typically relies on a closed-loop architecture where tracking loops are used to track the different signal components. Loop discriminators use correlator outputs to provide a measure of error between the actual and estimated signal parameters. In good signal-to-noise ratio (SNR) conditions, the discriminator outputs (Δ_{phase} and Δ_{code}) are guided close to zero by the tracking loops. However, as the SNR deteriorates, the standard deviation of the discriminator outputs increase (σ_{phase} and σ_{code}), lending themselves for analyzing the interference impact, as illustrated in Fig. 7. Based on the measurement results, the tracking stage is more likely to provide erroneous values with the interference mitigated as opposed to without mitigation. Although the operational range is extended similarly to the previous stages.

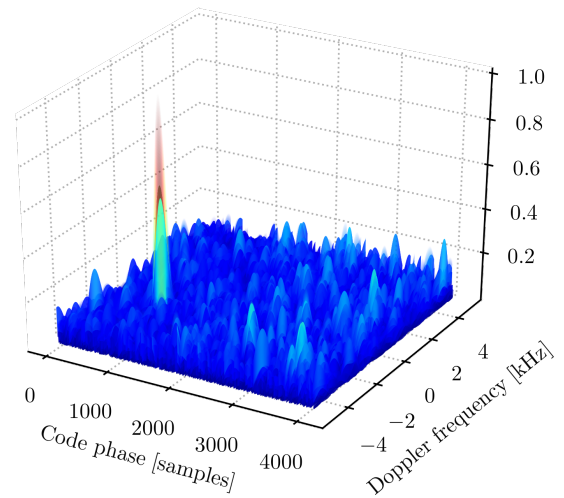
Besides the discriminator outputs, another aspect to analyze at this stage is the estimated carrier-to-noise ratio C/N_0 . The estimation of the C/N_0 depends on both the signal power estimation and the noise power estimation and several methods exist for these estimations [17]. The estimates are of course affected by interference and therefore they can also be an indication of adversarial interference [18]. The measured effect of FM interference on the estimation of C/N_0 with and without mitigation is plotted in Fig. 8. The C/N_0 measurement results are in line with the results presented in RF front-end and acquisition stages, i.e., the interference mitigation extends the normal C/N_0 estimation range by 30 dB to 40 dB.



(a) GPS acquisition without interference



(b) GPS acquisition with interference



(c) GPS acquisition with interference mitigation

Fig. 6. Comparison of the cross ambiguity function for GPS L1 acquisition search space without interference, with frequency-modulated interference (jammer-to-signal ratio of 50 dB) and with the interference suppressed.

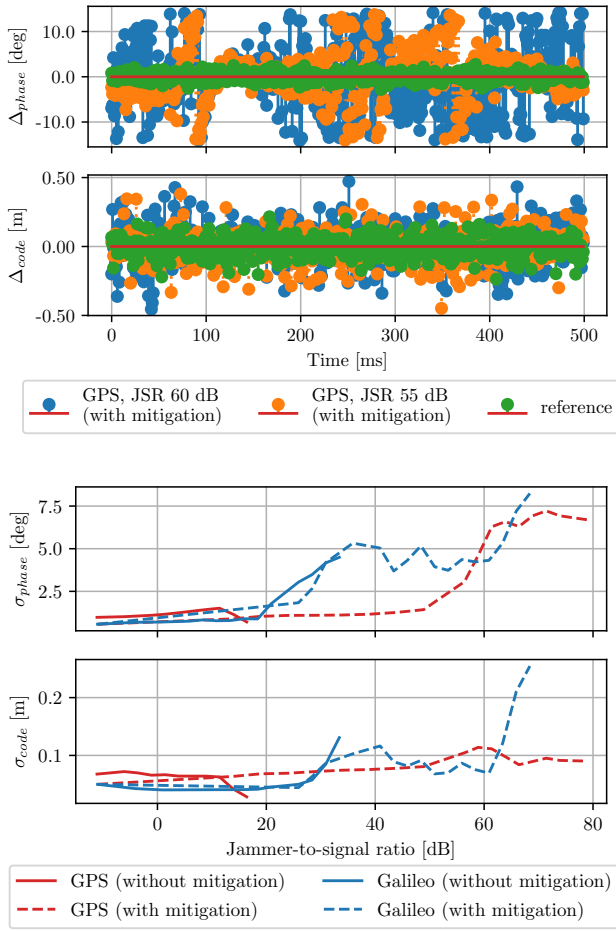


Fig. 7. Carrier and code discriminator outputs and standard deviations thereof. Phase-locked loop bandwidth is 15 Hz, delay-locked loop bandwidth is 2 Hz, and spacing between the early and late replicas is set to 0.5 code chips.

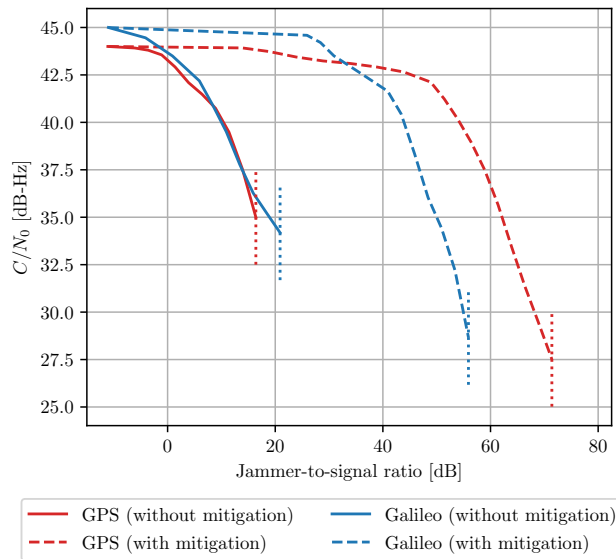


Fig. 8. Estimated C/N_0 values from the U-Blox receiver with and without interference mitigation. The dotted vertical lines indicate the jammer-to-signal ratio (JSR) from which on the receiver is unable to estimate C/N_0 .

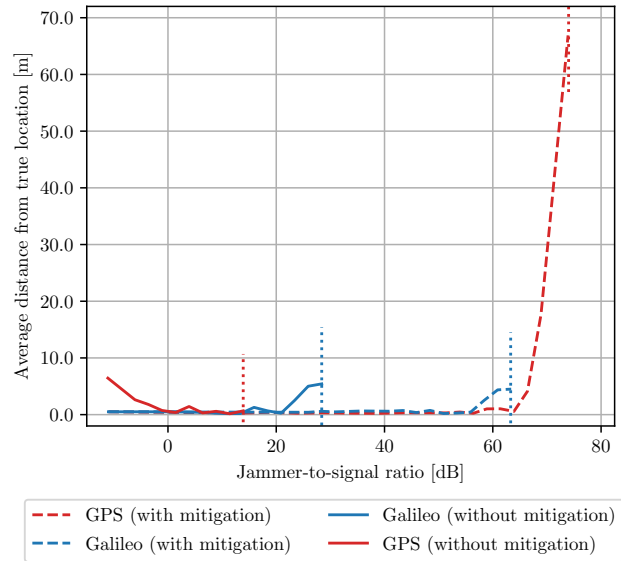


Fig. 9. GPS and Galileo positioning accuracy with regards to the jammer-to-signal ratio (JSR). Average of the U-Blox and GNSS-SDR distances is plotted for brevity as U-Blox and GNSS-SDR provide comparable accuracy. The dotted vertical lines indicate the JSR from which on the receivers are unable to acquire any position.

D. Positioning

If the GNSS signals can be acquired and tracked despite the interference, then the GNSS receiver can estimate its position. However, the position estimate may be degraded by the inaccuracies in pseudorange estimates caused by the interference. Figure 9 shows the average positioning accuracy of the U-Blox and GNSS-SDR receivers for both GPS L1 and Galileo E1 under interference with and without mitigation. It is evident that interference suppression allows the receivers to operate under much higher jammer-to-signal ratio (JSR), even though the effect is slightly different for GPS L1 and Galileo E1 positioning accuracy, presumably because of the different modulations used in GPS L1 and Galileo E1. During the 4 min measurements, poor SNR conditions tend to prevent the receivers from acquiring any positional fix rather than lead to very large positioning errors. In poor SNR conditions, the position is available for a fraction of the total measurement time whereas in good JSR conditions the position is available most of the time after acquiring the satellite parameters.

In a relatively small JSR range, the interference is severe enough to drastically decrease the GNSS receiver performance but not severe enough to force the receiver to prevent the acquisition of satellite signals or lose its lock on the satellite signals. For four such interference cases, the horizontal GPS positioning accuracy is illustrated in Fig. 10. The horizontal error ranges from couple meters to hundreds of meters. Such intermediate JSR ranges can perhaps be the most dangerous because of the difficulty to detect the interference [19]. In case the users fail to detect that the GNSS service is being interfered with, the positional inaccuracies may have a significant impact on the users' safety and security [20].

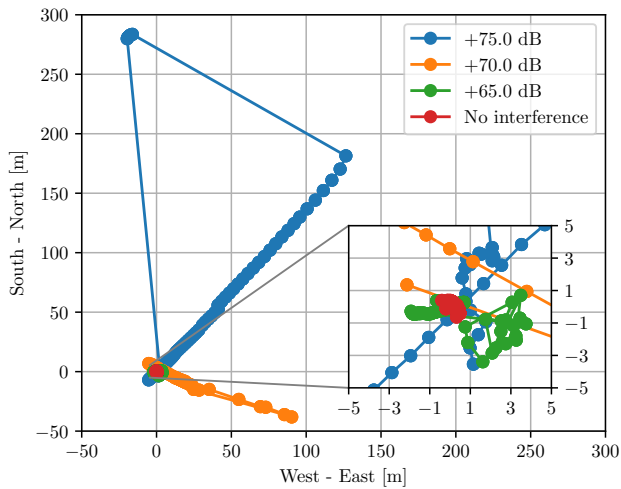


Fig. 10. GPS horizontal positioning accuracy with respect to the true coordinates without any interference and at three different jammer-to-signal ratios with interference mitigation. Each measurement spans 4 min.

V. CONCLUSIONS

Analog interference mitigation, as opposed to plain digital solutions, becomes necessary when the interference starts to limit the receiver's sensitivity due to the receiver's limited dynamic range. This is an outstanding issue in full-duplex (FD) radios but can also cause problems in co-located radios, especially when considering the typically weak global navigation satellite system (GNSS) transmissions as signals-of-interest. In this work, we analyzed how a digitally-assisted analog interference mitigation scheme affects GPS L1 and Galileo E1 reception in the presence of frequency-modulated interference, whereas the interference parameters are unknown to the receiver. We characterized the impact of interference and its mitigation on the radio-frequency (RF) front-end, acquisition, tracking, and positioning stages of GNSS receivers using a commercial off-the-shelf receiver and a separate open-source software-defined receiver.

The experimental results demonstrate considerable improvements in terms of preventing saturation in the RF front-end, cleaning up the acquisition search space, improving tracking accuracy and carrier-to-noise ratio estimates, and enhancing positioning accuracy for both GPS L1 and Galileo E1. The measurement results indicate that the operational jammer-to-signal ratio range of the GNSS receivers is extended proportionally to the amount of interference power suppression, for which one of the main limiting factors is the phase noise of the interference source. While the mitigation of periodic interference might have limited usage, extending such interference mitigation to suppress pseudorandom jamming could be desirable for differentiating between authorized and non-authorized receivers, for example, inside a FD radio shield.

REFERENCES

- [1] A. Sabharwal, P. Schniter, D. Guo, D. W. Bliss, S. Rangarajan, and R. Wichman, "In-band full-duplex wireless: Challenges and opportunities," *IEEE Journal on Selected Areas in Communications*, vol. 32, no. 9, pp. 1637–1652, Sep. 2014.
- [2] T. Riihonen, D. Korpi, O. Rantula, H. Rantanen, T. Saarelainen, and M. Valkama, "Inband full-duplex radio transceivers: A paradigm shift in tactical communications and electronic warfare?" *IEEE Communications Magazine*, vol. 55, no. 10, pp. 30–36, Oct. 2017.
- [3] K. Pärilin, T. Riihonen, R. Wichman, and D. Korpi, "Transferring the full-duplex radio technology from wireless networking to defense and security," in *Proc. 52nd Asilomar Conference on Signals, Systems and Computers*, Oct. 2018, pp. 2196–2201.
- [4] P. Ödling, O. P. Börjesson, T. Magesacher, and T. Nordström, "An approach to analog mitigation of RFI," *IEEE Journal on Selected Areas in Communications*, vol. 20, no. 5, pp. 974–986, Jun. 2002.
- [5] K. Pärilin and T. Riihonen, "Digitally assisted analog mitigation of narrowband periodic interference," in *Proc. International Symposium on Wireless Communication Systems*, Aug. 2019, pp. 682–686.
- [6] J. S. Warner and R. G. Johnston, "GPS spoofing countermeasures," *Homeland Security Journal*, vol. 25, no. 2, pp. 19–27, Jan. 2003.
- [7] R. H. Mitch, R. C. Dougherty, M. L. Psiaki, S. P. Powell, and B. W. O'Hanlon, "Signal characteristics of civil GPS jammers," in *Proc. Radionavigation Laboratory Conference*, Sep. 2011, pp. 1907–1919.
- [8] R. H. Mitch, M. L. Psiaki, S. P. Powell, and B. W. O'Hanlon, "Signal acquisition and tracking of chirp-style GPS jammers," in *Proc. 26th International Technical Meeting of the Satellite Division of The Institute of Navigation*, Sep. 2013, pp. 2893–2909.
- [9] K. D. Rao and M. Swamy, "New approach for suppression of FM jamming in GPS receivers," *IEEE Transactions on Aerospace and Electronic Systems*, vol. 42, no. 4, pp. 1464–1474, Oct. 2006.
- [10] M. Duarte, C. Dick, and A. Sabharwal, "Experiment-driven characterization of full-duplex wireless systems," *IEEE Transactions on Wireless Communications*, vol. 11, no. 12, pp. 4296–4307, Dec. 2012.
- [11] S. M. Kuo and D. R. Morgan, "Active noise control: A tutorial review," *Proceedings of the IEEE*, vol. 87, no. 6, pp. 943–973, Jun. 1999.
- [12] C. Fernández-Prades, J. Arribas, P. Closas, C. Avilés, and L. Esteve, "GNSS-SDR: An open source tool for researchers and developers," in *Proc. 24th International Technical Meeting of The Satellite Division of the Institute of Navigation*, Sep. 2001, pp. 780–794.
- [13] D. M. Akos and M. Pini, "Effect of sampling frequency on GNSS receiver performance," *Journal of The Institute of Navigation*, vol. 53, no. 2, pp. 85–95, Aug. 2006.
- [14] F. Bastide, D. Akos, C. Macabiau, and B. Roturier, "Automatic gain control (AGC) as an interference assessment tool," in *Proc. 16th International Technical Meeting of the Satellite Division of The Institute of Navigation*, Sep. 2003, pp. 2042–2053.
- [15] D. Akopian, "Fast FFT based GPS satellite acquisition methods," *IEE Proceedings—Radar, Sonar and Navigation*, vol. 152, no. 4, pp. 277–286, 2005.
- [16] D. Borio, F. Dovis, H. Kuusniemi, and L. L. Presti, "Impact and detection of GNSS jammers on consumer grade satellite navigation receivers," *Proceedings of the IEEE*, vol. 104, no. 6, pp. 1233–1245, Jun. 2016.
- [17] M. S. Sharawi, D. M. Akos, and D. N. Aloï, "GPS C/N_0 estimation in the presence of interference and limited quantization levels," *IEEE Transactions on Aerospace and Electronic Systems*, vol. 43, no. 1, pp. 227–238, Jan. 2007.
- [18] E. Axell, F. M. Eklöf, P. Johansson, M. Alexandersson, and D. M. Akos, "Jamming detection in GNSS receivers: Performance evaluation of field trials," *Journal of the Institute of Navigation*, vol. 62, no. 1, pp. 73–82, Mar. 2015.
- [19] F. Dovis, *GNSS Interference Threats and Countermeasures*. Artech House, 2015.
- [20] A. Grant, P. Williams, N. Ward, and S. Basker, "GPS jamming and the impact on maritime navigation," *The Journal of Navigation*, vol. 62, no. 2, pp. 173–187, Apr. 2009.